

Crystalline Structure Analysis of All-cellulose Nanocomposites Films Based on Corn and Wheat Straw

Hongxia BIAN (✉ [bxhia790311@gsau.edu.cn](mailto:bhxia790311@gsau.edu.cn))

Gansu Agricultural University

Yanyan Yang

Gansu Agricultural University

Peng Tu

Gansu Agricultural University

Research Article

Keywords: All-cellulose nanocomposite film (ANF), Crystalline index (CI), XRD, FTIR analysis

Posted Date: May 20th, 2021

DOI: <https://doi.org/10.21203/rs.3.rs-511111/v1>

License:   This work is licensed under a Creative Commons Attribution 4.0 International License.

[Read Full License](#)

Version of Record: A version of this preprint was published at BioResources on October 29th, 2021. See the published version at <https://doi.org/10.15376/biores.16.4.8353-8365>.

Abstract

The cellulose and nanocellulose which was extracted from corn straw and wheat straw was used to fabricate all-cellulose nanocomposites film (ANF). The crystal structure (CS) of ANFs was analyzed by X-ray diffraction (XRD) and Fourier transform infrared spectrometry (FTIR). The result shows that cellulose-I and cellulose-II are coexisting within regenerated cellulose films (RCF) and ANFs and can transfer each other with the change of nanocellulose content. The characteristics of cellulose transformation depend on the raw material and preparing method of cellulose. When cellulose is prepared from corn straw, under two preparing methods, the cellulose type tends to transform from cellulose-I to cellulose-II with low nanocellulose content and transform from cellulose-II to cellulose-I with high nanocellulose content. However, when cellulose is prepared from wheat straw, under extracting methods, the cellulose type tends to transform from cellulose-I to cellulose-II with nanocellulose content increase; under acid-alkali methods, the transformation is from cellulose-II to cellulose-I. The crystalline index (CI) of RCFs and ANFs is no obvious regularity, and the either content of cellulose-I or cellulose-II alone cannot determine the CI. Based on above result, the transformation characteristics of cellulose type should affect the property of ANFs, but further research methods and strategies are needed on what the effects are.

Introduction

As far as environmental protection is concerned, there is a growing demand for "environmentally friendly materials". Cellulose, as biodegradable and renewability natural materials, has come to the fore^[1]. Due to the huge reserve of cellulose, researchers can easily obtain it, process, and modify to produce a variety of cellulosic materials. Based on the purpose of replacing non-degradable packaging materials with degradable materials, it has attracted extensive attention in many researchers that cellulose is made into films. Further research on cellulose film products will inevitably accelerate environmental protection in industrial development and technological advancement today.

Crystal property, as one of the most important cellulose properties, can reflect many properties of cellulose products, especially mechanical strength^[2]. Studies have shown that cellulose owns five crystal structures, they are cellulose-I, II, III, IV and V, respectively^[3]. It has been reported that cellulose-I and cellulose-II appeared commonly in cellulosic films. Such as, the structure of the films, which were made up of valonia ventricose, ramie and bacterial cellulose and prepared in different ways by C. Y. Lang and R. H. Marchessault, is cellulose I^[4]. The CS of cellulose powder was transformed from cellulose-I to cellulose-II after treating with 5–10 wt% NaOH^[5]. Due to the intermolecular and intramolecular hydrogen-bonding of cellulose macro-molecules, the CS of all cellulose materials is stable and tough. Moreover, primary hydrogen bond is O_2-H-O_6 in cellulose-I, and O_2-H-O_6 , O_2-H-O_2 , O_6-H-O_6 in cellulose-II. Two cellulose macro-molecules chains parallel to each other are connected by hydrogen bonds and formed a three-dimensional network structure^[6]. So, the CI of cellulosic materials and cellulose derivatives is higher than straight-chain polymers. With the popularity of the concept of "sustainable economic development" in today society, researchers expected to use cellulosic films instead of non-degradable

materials [7]. Therefore, the studies on cellulose CI and CS on cellulose films will help that the researchers improve their mechanical properties better.

XRD and FTIR were used to analyze ANFs and RCFs [8]. Due to the advantage of rapid detection, simple operation, convenient data processing, XRD has a wide range of application. The spectrum information can not only realize the conventional microscope to determine the phase, but also has a "perspective eye" to see whether there are defects inside the crystal. The advantages of FTIR are the fast analysis, simple operation, can simultaneously determine a variety of functional groups, good selectivity, high sensitivity, less sample damage, can determine the crystal type of cellulose film by the shifting of characteristic peaks position in the spectrum.

There are several ways to calculate the CI of cellulose, and use the spectrum of XRD and FTIR is the main way. Usually, the CI is obtained by X-ray diffraction, which refers to as CI(XD), is calculated by the method of Jayme and Knolle, and the CI is obtained by FTIR, which refers to as CI(IR), is obtained by absorbance ratios, such as $A_{1431,1419}/A_{897,894}$ and $A_{1263}/A_{1202,1200}$ [5]. The empirical method using the ratio of intensity of diffractogram peak at the position of the crystal plane(0 0 2) ($2\theta = 22.6^\circ$ for cellulose-I and $2\theta = 21.7^\circ$ for cellulose-II) and amorphous background ($2\theta = 19.0^\circ$ for cellulose-I, $2\theta = 16.0^\circ$ for cellulose-II) also can be used to calculate the CI, and the formula is as follows [9]:

$$CI\% = \frac{I_{002} - I_{am}}{I_{002}} \%$$

Of course, the CI(XD) also can be calculated by the ratio of the diffraction peak area of cellulose-I (or cellulose-II) and total peak area. Besides, using the pure sample method for calculating CI. A diffraction peak intensity of 100% crystalline sample (I_{a100}) of the substance (or 100% amorphous sample, I_{c100}) and diffraction peak intensity of the sample can be measured, and used I_{c100} (I_{a100}) and I_c (I_a) characterized respectively. The relationship is shown by following this equation [10]:

$$CI\% = \frac{I_c}{I_{c100}} \%$$

In this study, the cellulose and nanocellulose, which are used to prepared ANFs and RCFs, are all derived from agricultural residues, wheat straw and corn straw which are rich in sources and easy to obtain, and are environmentally friendly. The preparing method of cellulose, nanocellulose, ANFs and RCFs in this paper is referred to the literature [11]. Basing the different material and preparing method of cellulose, the crystallization characters of ANFs and RCFs will be analyzed and compared. The CS and CI of material is closely related to its mechanical properties, so, the research on the CS and CI of cellulose products plays an extremely important role in expanding the use of cellulose-based materials in daily life.

Experiment

Materials

Cellulose, which came from agricultural residual corn and wheat straw, were prepared by acid-based method and extracting method, respectively. Nanocellulose, which also came from corn and wheat straw, were prepared by TEMPO oxidation method. The DMAc (99.8%) and LiCl, which was obtained from Shanghai Zhanyun Chemical Industry Co. Ltd, were used to dissolve cellulose.

Methods

The preparing method on cellulose, nanocellulose and all-cellulose nanocomposite film all refers to literature^[11]. The simple statement just shows the correlation between the preparing method and the crystallization process.

The cellulose was extracted by two different methods. One method, which is referred to acid-alkali method, is using acid and alkali to extract cellulose and taking ultrasonic as an auxiliary. The other, which is referred to extracting method, is using Soxhlet extractor to take off the fat, wax, etc. Nanocellulose was prepared by TEMPO oxidation and should be include many carboxyls. ANFs were prepared by regenerating the cellulose which was dissolved using the DMAc/LiCl solution system, and added nanocellulose of 0.1 %, 1.5 %, 3.0 %, respectively, to strengthen. In the process of fabricating ANF, cellulose and nanocellulose both came from same straw. That is if cellulose came from wheat straw, nanocellulose also came from wheat straw.

Characterizations

X-ray diffraction (XRD)

The XRD was used to investigate crystalline type, calculate CI. The XRD, which was used in the study, is a X-ray diffractometer (Puxitongyun XD-2) with nickel-filtered Cu K α radiation($\lambda = 1.540\text{nm}$). The operating voltage and current are 40 kV and 30mA, respectively, scanning step and range are $0.01^\circ\text{min}^{-1}$ and $10-45^\circ$.

Fourier transform infrared spectrometry (FTIR)

The FTIR spectrum was also used to calculate CI and analyze the crystal structure and type in cellulose. The FTIR used measurement is a Thermofisher Nicolet IS 50. The characteristic peaks' ratios were used to obtain CI, and it can obtain more accurate CI than other ways. All spectra were recorded with an accumulation of 64 scans, resolution of 4 cm^{-1} , in the range from 4000 cm^{-1} to 400 cm^{-1} . Three different measurements for each sample were evaluated, and the average value was calculated.

Results And Discussion

XRD analysis

All measurement results of XRD were fitted by peak separation method [12]. The XRD diffraction patterns of ANFs and RCFs, which original materials came from corn straw and was fabricated by dissolving cellulose prepared by extraction method and acid-alkali method, respectively, and adding different concentration of nanocellulose, were shown in Fig. 1. The diffraction pattern range of ANFs and RCFs is mainly from 10° to 30° . In Fig. 1a, the crystal peaks appear at $2\theta = 16.1^\circ$ - 17.5° (1 0-1), $2\theta = 20.8^\circ$ - 21.9° (0 0 2), and indicates that the crystal coexistence state of cellulose-I and cellulose-II in ANFs and RCFs [13, 14]. Compared with the primary and secondary diffraction peaks at $2\theta = 21.0^\circ$ and 16.5° of RCF, the primary and secondary diffraction peaks of $2\theta = 21.9^\circ$ and 17.5° shift toward right when the concentration of nanocellulose is 0.1% in the ANF. The phenomenon indicates that the content of cellulose-I was significantly reduced and cellulose-II was increased gradually when the concentration of added nanocellulose is 0.1% and further indicates the transformation of cellulose-I to cellulose-II in the ANF [15]. This may be caused by the formation of holes in the sample after ultrasonic treatment during the preparation of cellulose, and the formation of a certain molecular orientation due to a small amount of nanocellulose, which further deepened the trend of conversion to cellulose-II [11]. However, the secondary diffraction peak of $2\theta = 17.5^\circ$ shift toward the $2\theta = 16.2^\circ$ when the concentration of nanocellulose reached 1.5%. It means that the crystal type of ANF transformed from cellulose-II to cellulose-I again. When the concentration of nanocellulose reached 3%, there was no change in the crystal type of ANF, which remained cellulose-I and indicates that the crystalline type of nanocellulose is cellulose-I. The overall CS of ANF changes from cellulose-II to cellulose-I when the concentration of nanocellulose reached 1.5%. Therefore, the crystal type of ANF does not change when the concentration of nanocellulose continued to increase.

When the cellulose was prepared by acid-alkali method, the diffraction pattern of ACFs and RCF was shown in Fig. 1b. Compared with the diffraction patterns of the ANFs and RCF which cellulose was prepared by extracting method, the primary and secondary peaks at $2\theta = 16.8^\circ$, 21.8° appeared in RCF, and this indicated the coexistence of cellulose-I and cellulose-II. This is consistent with the crystal type of ANF prepared by extracting method. Similarly, the positions of the primary and secondary peaks at $2\theta = 17.3^\circ$, 21.9° shift to the right when the concentration of nanocellulose is 0.1% and it suggests that the CS changes from cellulose-I to cellulose-II. Similar to the ANF which cellulose was prepared by extracting method, the $2\theta = 16.0^\circ$ indicated that crystal type transformed from cellulose-II to cellulose-I when the nanocellulose concentration is 1.5%. The crystal type of ANF did not change when the concentration of nanocellulose was doubled. Differently, when the concentration of nanocellulose is 3.0%, the intensity of the peak at $2\theta = 21.7^\circ$ is significantly increase and indicates that the content of cellulose-II is increased. This shift could be because that cellulose was soaked by sodium hydroxide (8%) during preparation process, and alkali treatment could convert cellulose-I to cellulose-II. In the process of mercerization, the whole fiber is transformed into the swollen state, the assembly and direction of microfibrils are completely broken, and the parallel chain structure of cellulose-I is transformed into the anti-parallel chain structure of cellulose-II [16].

The XRD diffraction patterns of ANFs and RCFs, which original materials came from wheat straw and was fabricated by dissolving cellulose prepared by extraction method and acid-alkali method, respectively, and adding different concentration of nanocellulose, were shown in Fig. 2. The range of the diffraction pattern of ANFs is mainly from 10° to 30° . As shown in Fig. 2a, the appearance of the primary peak and the secondary at $2\theta = 17.2^\circ$ and $2\theta = 20.6^\circ$ respectively, indicates the existence of cellulose-I. When the concentration of nanocellulose is 0.1%, the crystalline type transforms from cellulose-I to cellulose-II gradually, and the appearance of the primary and secondary peaks at $2\theta = 16.4^\circ$ and $2\theta = 21.6^\circ$ confirmed this transformation. When the concentration of nanocellulose continues to increase, the crystal type of ANFs does not change. The intensity of primary peaks at $2\theta = 21.2^\circ$ - 21.3° is slightly higher than the secondary peaks at $2\theta = 16.6^\circ$ - 16.8° . It may be caused that the structure of cellulose-I of ANFs was destroyed through the action of alkalization and ultrasound, and part of the crystalline region was rearranged into cellulose-II.

As shown in Fig. 2b, compared with the diffraction patterns of ANFs and RCFs from corn straw, the changing of this diffraction pattern in ANFs of wheat straw is different. The primary and secondary peaks at $2\theta = 16.2^\circ$, 21.4° confirmed that cellulose-I and cellulose-II both present in RCF. When the concentration of nanocellulose is 0.1%, the crystal type of ANF is consistent with RCF. When the concentration of nanocellulose reached 1.5%, the primary peak at $2\theta = 22.1^\circ$ (002) appears. It proves that the crystalline type of cellulose is transformed from cellulose-II to cellulose-I. When the concentration of nanocellulose reached 3.0%, the primary and secondary peaks at $2\theta = 20.9^\circ$, 16.3° appear. It again proves that the crystal type of ANFs changes from cellulose-I to cellulose-II.

FTIR analysis

The FTIR spectrum of RCFs and ANFs with different concentration nanocellulose and cellulose extracted by extracting method from corn straw are shown Fig. 3. As shown in Fig. 3a, the bands at 3347 cm^{-1} assigned as -OH stretching vibration is shifted to lower wavenumbers 3338 cm^{-1} . The XRD patterns of the RCF of corn straw prepared by the extracting method is cellulose-I and cellulose-II are coexisting. There is a wide absorptive peak at 3338 cm^{-1} , also proves that cellulose-I and cellulose-II are coexisting in the RCF. The band at 2891 cm^{-1} is assigned as -CH stretching in cellulose-II^[17]. From the infrared spectrum, the absorption peak at 2891 cm^{-1} gradually changes from a flat peak to a sharp peak with the increasing of nanocellulose concentration. This phenomenon indicates a gradual transition from cellulose-I to cellulose-II.

As shown in Fig. 3b, the absorbance intensity at 1419 cm^{-1} assigned as symmetric -CH₂ bending is shifted to higher wavenumbers 1421 cm^{-1} , when the concentration of nanocellulose is 1.5%. It indicates that the cellulose-II transforms to cellulose-I^[18]. With the increasing of the nanocellulose concentration, the intensity of the absorption peak at 1367 cm^{-1} increases, and the width of the absorption peak gradually narrows. It may be caused by the content of cellulose-I in the CS of ANFs increase due to the addition of nanocellulose. The band at 1262 cm^{-1} assigned as -COH in the plane at C-2 and C-3 in

cellulose-I and cellulose-II, and indicates the coexistence of cellulose-I and cellulose-II in ANFs and RCFs. The bands at 1157 cm^{-1} , 1015 cm^{-1} are assigned as C-O-C stretching in cellulose-II and C-O stretching, respectively. Similarly, with the increase of nanocellulose content, these peaks' pattern changes from flat peak to sharp peak. It indicates that the region of cellulose-II in the CS of ANFs gradually concentrates in a certain part. The band at 992 cm^{-1} assigned C-O stretching at C-6, is shifted to the lower wavenumber at 990 cm^{-1} . It suggests that the transformation from cellulose-II to cellulose-I of CS in ANFs. The band at 896 cm^{-1} is assigned as β -glycosidic linkage for cellulose-I, and shifts to 894 cm^{-1} when the concentration of nanocellulose is 0.1%. It indicates that the crystalline type of ANFs changes from cellulose-II to cellulose-I. The absorption band moves from 894 cm^{-1} to 895 cm^{-1} when the concentration of nanocellulose is 3.0%. It indicates there is a transition from cellulose-I to cellulose-II in ANFs. This phenomenon is consistent with the results obtained by XRD.

The FTIR spectrum of RCFs and ANFs with different nanocellulose concentration and the cellulose was prepared by acid-alkali method from corn straw are shown in Fig. 4. In Fig. 4a, there is a large absorption peak between 3643 cm^{-1} and 3013 cm^{-1} . The absorption intensity of peak reaches the maximum when the position is 3322 cm^{-1} . There is also a broadening absorption peak between 2977 cm^{-1} and 2784 cm^{-1} . The absorption intensity of peak reaches the maximum when the position is 2894 cm^{-1} . The bands at 3322 cm^{-1} , 2894 cm^{-1} are assigned as -OH stretching vibration and -CH stretching in cellulose-II, respectively [19].

As shown in Fig. 4b, the absorbance intensity at 1419 cm^{-1} is assigned as symmetric -CH₂ bending of cellulose-II. The peak at 1422 cm^{-1} is shifted to 1420 cm^{-1} when the concentration of nanocellulose is 0.1%, and it indicated that the crystalline type of RCF gradually transfers to cellulose-II. The band at 1317 cm^{-1} is assigned as -CH₂ wagging at C-6. The position of the peaks at 1315 cm^{-1} appears a weak absorption peak in RCF, and it suggests that cellulose-I and cellulose-II all exist in RCF. When the concentration of nanocellulose was 0.1% and 1.5%, the peak at 1315 cm^{-1} was shifted to 1312 cm^{-1} , which might be due to the use of ultrasonic treatment in the preparing cellulose process, so that the partial of CS was destroyed and reconstituted, and tended to be cellulose-II. The band at 992 cm^{-1} also is shifted to 990 cm^{-1} when the concentration of nanocellulose is 0.1%. It suggests that cellulose-II transforms to cellulose-I in ANFs. The absorbance intensity at 895 cm^{-1} is assigned as antisymmetrical out of phase stretching of cellulose-II, and the peak at 895 cm^{-1} shifts to 897 cm^{-1} when the concentration of nanocellulose is 1.5%. It indicates that the crystalline type of ANFs gradually transforms to cellulose-I. Similarly, when the concentration of nanocellulose is 3%, the absorptive peaks at 1420 cm^{-1} , 1312 cm^{-1} , 990 cm^{-1} , 897 cm^{-1} are shifted to higher wavenumbers at 1422 cm^{-1} , 1315 cm^{-1} , 991 cm^{-1} , 895 cm^{-1} , and it proves again that cellulose-I transforms to cellulose-II in ANFs. This phenomenon is corresponding to Fig. 1b.

The FTIR spectrums of RCFs and ANFs with different concentration nanocellulose and cellulose treated by extracting method from wheat straw are shown in Fig. 5. From Fig. 5a, the bands at 3346 cm^{-1} shows

-OH stretching of intramolecular hydrogen bonds. This indicates that cellulose-I existed in ANFs which obtained from wheat straw. The bands at 2891 cm^{-1} manifests -CH stretching of cellulose-II. Meanwhile, the position of peak at 2916 cm^{-1} appeared a shoulder peak is assigned as -CH stretching [20].

As shown in Fig. 5b, the band at 1635 cm^{-1} is assigned as -OH bending about water. The bands at 1421, 1367, 1316 cm^{-1} are assigned as $-\text{CH}_2$ bending, -CH bending and $-\text{CH}_2$ wagging at C-6, and indicates that cellulose-I and cellulose-II coexist in ANF and RCF [21]. The absorption peaks at 1199 cm^{-1} are assigned as -COH bending at C-6 in cellulose-II. The absorbance intensity at 1156 cm^{-1} is assigned as C-O-C stretching vibration in cellulose-II. The absorption peaks at 1015 cm^{-1} and 990 cm^{-1} are assigned as C-O stretching at C-6 in cellulose-II. The bands at 896 cm^{-1} are assigned as -COC at β -glycosidic linkage in cellulose-I. When the concentration of nanocellulose was 3.0%, it is worth noting that the intensity of absorption peaks in the figure all increase.

The FTIR spectrums of RCFs and ANFs with different concentration nanocellulose and cellulose treated by acid-alkali method from wheat straw are shown in Fig. 6. From Fig. 6a, the bands at 3338 cm^{-1} shows -OH stretching of intramolecular hydrogen bonds. This indicates that cellulose-I existed in ANFs which obtains from wheat straw. The bands at 2891 cm^{-1} manifests -CH stretching of cellulose-II. The position of peak at 2916 cm^{-1} disappears when the concentration of nanocellulose is 1.5% and 3.0%.

As shown in Fig. 6b, the band at 1633 cm^{-1} is assigned as -OH bending about water. The bands at 1423 cm^{-1} are assigned as $-\text{CH}_2$ bending and indicates that cellulose-I exists in ANFs and CRF. The peak at 1368 cm^{-1} in CRF shifts to 1370 cm^{-1} when the concentration of nanocellulose is 0.1%. This phenomenon suggests that crystalline type transforms from cellulose-I to cellulose-II. When the concentration of nanocellulose increase from 0.1–1.5% and then to 3.0%, the absorption peak also shifts from 1370 cm^{-1} to 1368 cm^{-1} and then to 1360 cm^{-1} . This indicates that crystalline type of ANFs transforms cellulose-II to cellulose-I. The bands at 1314 cm^{-1} are assigned as $-\text{CH}_2$ wagging at C-6, and indicates that cellulose-II exists in ANF and CRF. The absorption peaks at 1199 cm^{-1} are assigned as -COH bending at C-6 in cellulose-II. The absorbance intensity at 1156 cm^{-1} is assigned as C-O-C stretching vibration in cellulose-II. The absorption peaks at 1015 cm^{-1} and 990 cm^{-1} are assigned as C-O stretching at C-6 in cellulose-II. The bands at 896 cm^{-1} are assigned as -COC at β -glycosidic linkage in cellulose-I. When the concentration of nanocellulose was 0.1%, it is worth noting that the intensity of absorption peaks in the figure all increase.

Crystallinity index (CI) analysis

In this paper, the calculation equation of CI on X-ray diffraction is as follows:

$$CI = \frac{A}{B} \times 100\%$$

where A is the area of crystalline peaks; B is the area of all peaks (crystalline and amorphous).

The RCFs' and ANFs' CI of corn straw and wheat straw is shown in Table 1, among which the cellulose is prepared by the acid-alkali and extracting method, respectively. CI is one of key factor to determine the films' mechanical property, therefore, the analysis of CI is very important to understand the mechanical properties of films. The CI of RCF which cellulose was prepared by acid-alkali method from corn straw is 63.6%, and it is higher than the RCF which cellulose was prepared by extracting method from corn straw. The CI of RCF obtained from wheat straw is also the same. In the ANFs which cellulose prepared by acid-alkali method from corn straw, the CI increases with the increase of the nanocellulose concentration. When the nanocellulose concentration is 3.0%, the CI of ANF is 67.9%. In the ANFs which cellulose prepared by extracting method from corn straw, when the ANFs with concentrations of 0.1% and 1.5% nanocellulose, the CI increased to 71.9%. Differently, when the concentration of nanocellulose is 3.0%, the CI of ANF decreased to 58.6%.

Table 1
The CI of all kinds of ANFs

Material	Method of preparing cellulose	Nanocellulose content			
		RCF	0.1%	1.5%	3%
Corn straw	Acid-alkali method	63.6	59.6	64.7	67.9
	Extracting method	58.5	68.0	71.9	58.6
Wheat straw	Acid-alkali method	72.7	60.9	58.5	52.1
	Extracting method	56.9	66.9	58.1	63.9

In the ANFs which cellulose prepared by acid-alkali method from wheat straw, the opposite phenomenon appears. The CI decreased to 52.1%, when the nanocellulose content is 3.0%. This may be the ANFs absorbed H_2O molecules in the storage process, and H_2O molecules gradually entered the crystalline region from the amorphous region, destroying the part of crystalline structure and reducing the CI of ANFs [22]. When the concentration of nanocellulose is 3.0%, the CI of ANFs which cellulose prepared by extracting method from wheat straw increases to 63.9%. On the whole, the addition of nanocellulose can improve the CI of ANFs, and it is expected that the mechanical properties of ANFs will be strengthened.

Conclusion

The CS and CI of ANFs, which were fabricated using the cellulose and nanocellulose extracted from wheat and corn straw, were analyzed in the study. The effect of the preparing method of cellulose and original material on CS, and CI in ANFs has been discussed. Through the overall analysis of this research, with increasing of nanocellulose, the CS of all ANFs which cellulose was obtained from corn straw transformed from cellulose-I to cellulose-II when the concentration of nanocellulose is 0.1%, but when the concentration increased to 3.0%, the crystal type of cellulose-II partly transformed to cellulose-I, too. Differently, in the ANFs which cellulose was obtained by extracting method from wheat straw, the CS only

transformed from cellulose-I to cellulose-II when the concentration of nanocellulose is 0.1%, but in the ANFs which cellulose was obtained by acid-alkali method from wheat straw, it exists the phenomenon of cellulose-II transformed to cellulose-I when the concentration of nanocellulose is 1.5%.

Deserve to be mentioned in the FTIR spectra, the bands at 3347, 1419, 992, 895 cm^{-1} were shifted to 3338, 1421, 990, 894 cm^{-1} , respectively, and it indicated that cellulose-II were transformed to cellulose-I in ANFs which cellulose was obtained by extracting method from corn straw. the absorption peaks at 1420, 1312, 990, 897 cm^{-1} were shifted to higher wave numbers at 1422, 1315, 991, 895 cm^{-1} , respectively, and this suggested that cellulose-I were transformed to cellulose-II in ANFs which cellulose was obtained by acid-alkali method from corn straw. The appearance of absorption peaks at 3346, 2891, 2916, 1421, 1367, 1316, 896 cm^{-1} indicated that cellulose-I and cellulose-II coexistence in wheat straw films. By calculating the CI of ANF, the CI of RCF obtained from corn straw prepared by the acid-alkali method is 63.6%, this is higher than prepared by extracting method of corn straw. The CI of RCF obtained from wheat straw is also the same. In the ANF of corn straw which prepared by acid-alkali method, the CI of ANF increases to 67.9% when the concentration of nanocellulose increase to 3.0%. On the whole, the addition of nanocellulose can improve the CI of ANFs and enhance mechanical properties.

References

1. Hai LV, Kim HC, Kafy A, Zhai L, Kim JW, Kim J (2017) Green all-cellulose nanocomposites made with cellulose nanofibers reinforced in dissolved cellulose matrix without heat treatment. *Cellulose* 24:3301–3313. <https://doi.org/10.1007/s10570-017-1333-7>
2. Li Q, Chen W, Li Y, Guo X, Song S, Wang Q, Liu Y, Li J, Yu H (2016) Comparative study of the structure, mechanical and thermomechanical properties of cellulose nanopapers with different thickness. *Cellulose* 23:1375–1382. <https://doi.org/10.1007/s10570-016-0857-6>
3. Dong XM, Gray DG (1997) Induced circular dichroism of isotropic and magnetically-oriented chiral nematic suspensions of cellulose crystallites. *Langmuir* 13:3029–3034. <https://doi.org/10.1021/la9610462>
4. Liang CY, Marchessault RH (1959) Infrared spectra of crystalline polysaccharides. I. Hydrogen bonds in native celluloses. *Journal of polymer science* 37:385–395. <https://doi.org/10.1002/pol.1959.1203713209>
5. Oh SY, Yoo DI, Shin Y, Kim HC, Kim HY, Chung YS, Park WH, Youk JH (2005) Crystalline structure analysis of cellulose treated with sodium hydroxide and carbon dioxide by means of X-ray diffraction and FTIR spectroscopy. *Carbohydr Res* 340:2376–2391. <https://doi.org/10.1016/j.carres.2005.08.007>
6. Yue YY (2011) A comparative study of cellulose I and II and fibers and nanocrystals[D]. LSU Master's Theses, p 764
7. Escursell S, Llorach P, Roncero MB (2021) Sustainability in e-commerce packaging: A review. *J Clean Prod*, 280. <https://doi.org/10.1016/j.jclepro.2020.124314>

8. Angelin Vinodhini P, Sangeetha K, Thandapani G, Sudha PN, Jayachandran V, Sukumaran A (2017) FTIR, XRD and DSC studies of nanochitosan, cellulose acetate and polyethylene glycol blend ultrafiltration membranes. *Int J Biol Macromol* 104:1721–1729. <https://doi.org/10.1016/j.ijbiomac.2017.03.122>
9. Nelson ML, O'Connor RT (1964) Relation of certain infrared bands to cellulose crystallinity and crystal lattice type. Part II. A new infrared ratio for estimation of crystallinity in celluloses I and II. *J Appl Polym Sci* 8:1325–1341. <https://doi.org/10.1002/app.1964.070080323>
10. Huang JW, Li Z (2012) X-ray diffraction of polycrystalline materials-experimental methods, principles and applications[M]. Metallurgical Industry press, Beijing
11. Bian HX, Tu P, Chen JY (2020) Fabrication of all-cellulose nanocomposites from corn stalk. *J Sci Food Agric* 100:4390–4399. <https://doi.org/10.1002/jsfa.10476>
12. Park S, Baker JO, Himmel ME, Parilla PP, Johnson DK, Cellulose crystallinity index: Measurement techniques and their impact on interpreting cellulose performance [J]. *Biotechnol Biofuels*, 2010 (3): 1–10. <https://doi.org/10.1186/1754-6834-3-10>
13. Zhao JQ, He X, Wang Y, Zhang W, Zhang X, Zhang X, Deng Y, Lu C (2014) Reinforcement of all-cellulose nanocomposite films using native cellulose nanofibrils. *Carbohydr Polym* 104:143–150. <https://doi.org/10.1016/j.carbpol.2014.01.007>
14. Nishiyama Y, Langan P, Chanzy H (2002) Crystal structure and hydrogen bonding system in cellulose I β from synchrotron X-ray and neutron fiber diffraction. *J Am Chem Soc* 124:9074–9082. <https://doi.org/10.1021/ja037055w>
15. Wang HY, Li SY, Wu TT, Wang XX, Cheng XD, D. D.Li (2019) A Comparative Study on the Characterization of Nanofibers with Cellulose I, I/II, and II Polymorphs from Wood. *Polymers* 11:153. <https://doi.org/10.3390/polym11010153>
16. Manjunath BR, Peacock N (1972) Chain conformations in cellulose I and cellulose II. *Applied polymer* 16:1305–1308. <https://doi.org/10.1002/app.1972.070160520>
17. Higgins HG, Stewart CM, Harrington KJ (1961) Infrared spectra of cellulose and related polysaccharides. *Journal of polymer science* 51:59–84. <https://doi.org/10.1002/pol.1961.1205115505>
18. Liang CY, Marchessault RH (1959) Infrared spectra of crystalline polysaccharides. II. Native celluloses in the region from 640 to 1700 cm^{-1} . *Journal of polymer science* 39:269–278. <https://doi.org/10.1002/pol.1959.1203913521>
19. Yukako H, Eiji T, Tetsuo K (2017) Characterization of Individual Hydrogen Bonds in Crystalline Regenerated Cellulose Using Resolved Polarized FTIR Spectra. *ACS Omega* 2:1469–1476. <https://doi.org/10.1021/acsomega.6b00364>
20. Liang CY, Marchessault RH (1959) Infrared spectra of crystalline polysaccharides. I. Hydrogen bonds in native celluloses. *Journal of polymer science* 37:385–395. <https://doi.org/10.1002/pol.1959.1203713209>

21. Nelson ML, O'Connor RT (1964) Relation of certain infrared bands to cellulose crystallinity and crystal latticed type. Part I. Spectra of lattice types I, II, III and of amorphous cellulose. Journal of applied science 8:1311–1324. <https://doi.org/10.1002/app.1964.070080322>
22. Agarwal UP, Ralph SA, Baez C, Reiner RS, Verrill SP (2017) Effect of sample moisture content on XRD-estimated cellulose crystallinity index and crystallite size. Cellulose 24:1971–1984. <https://doi.org/10.1007/s10570-017-1259-0>

Figures

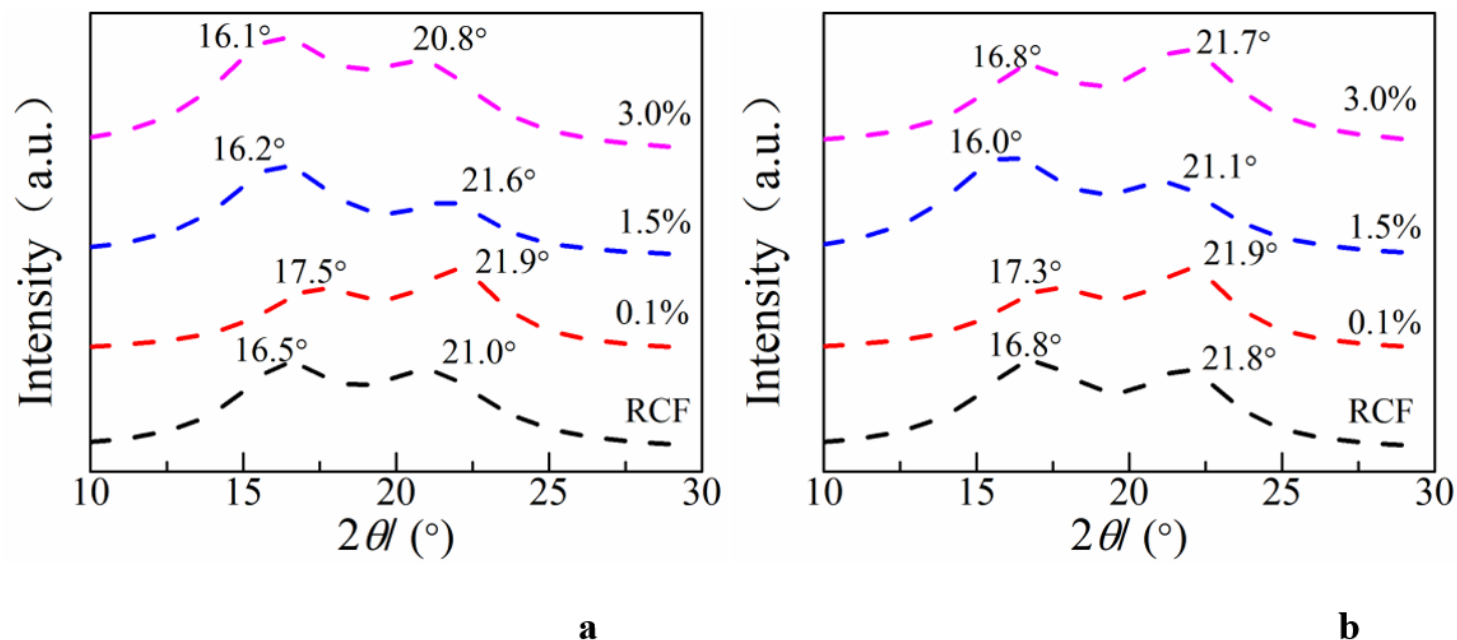


Figure 1

The XRD diffraction pattern of ANFs and RCFs which original material came from corn straw and the cellulose were extracted by a) extracting method and b) acid-alkali method

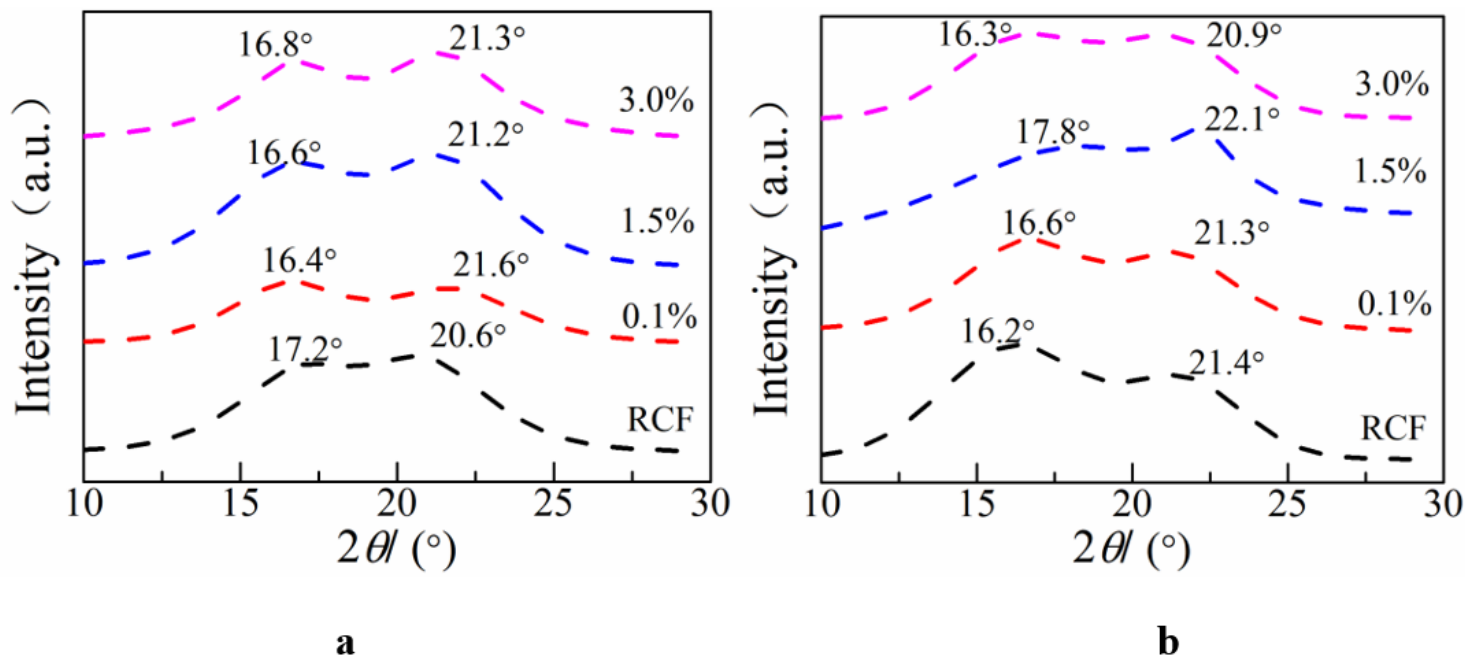


Figure 2

The XRD diffraction pattern of ANFs and RCFs which original material came from wheat straw and the cellulose were extracted by a) extracting method and b) acid-alkali method

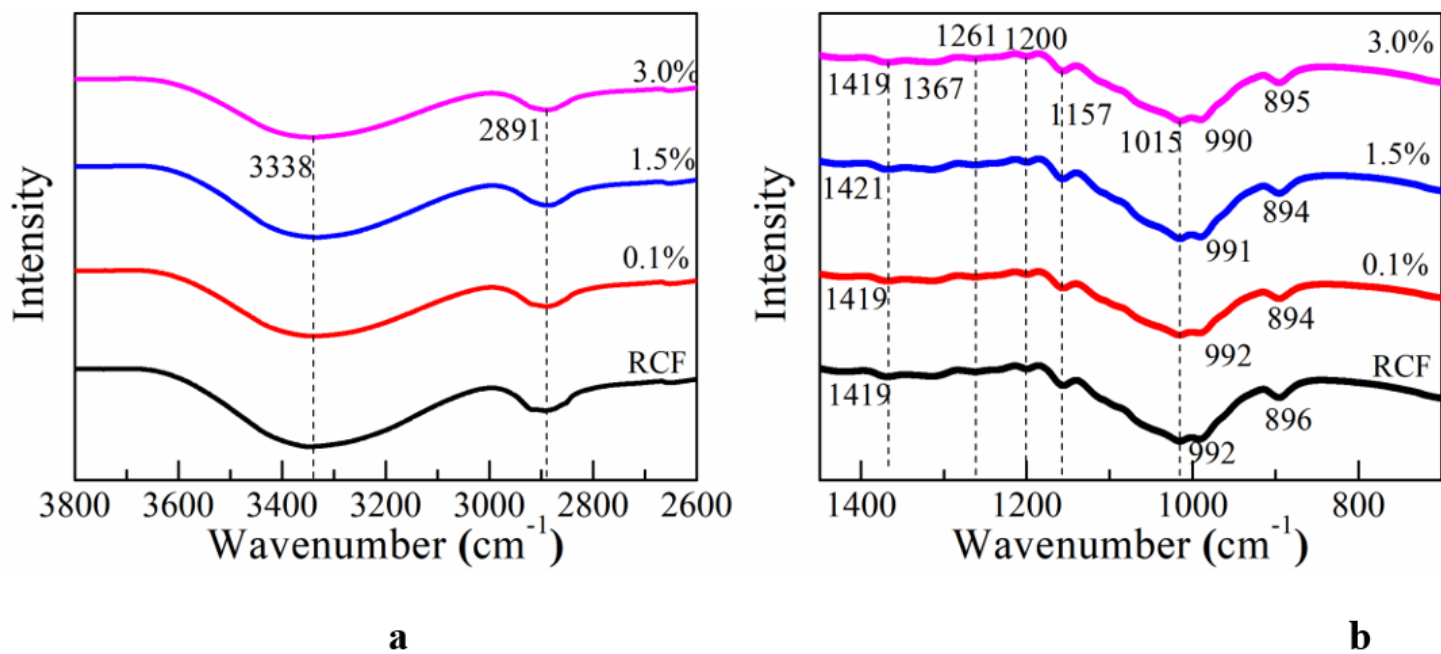
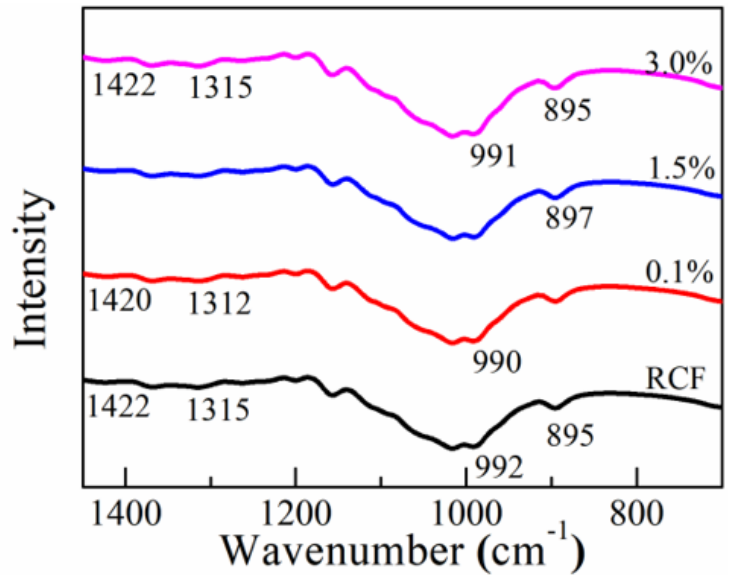
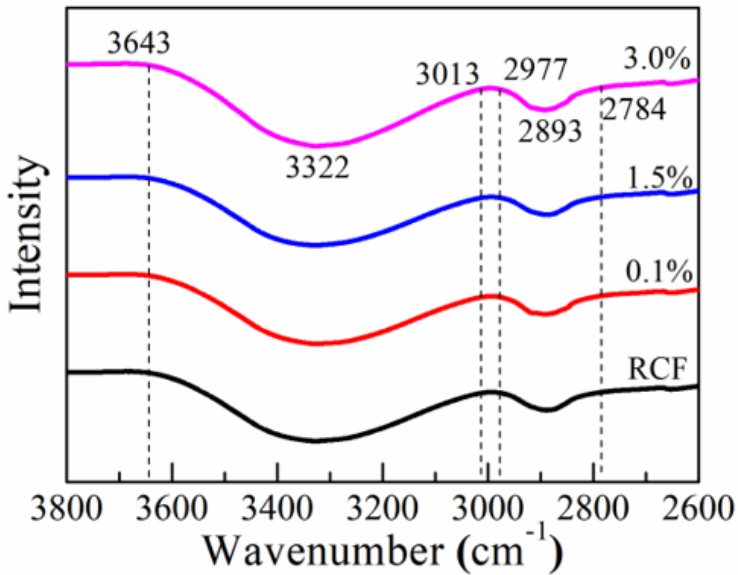


Figure 3

The FTIR spectrum of ANFs and RCFs which original material came from corn straw and the cellulose were prepared by extracting method a) 3800-2600 cm⁻¹, b) 700-1450 cm⁻¹

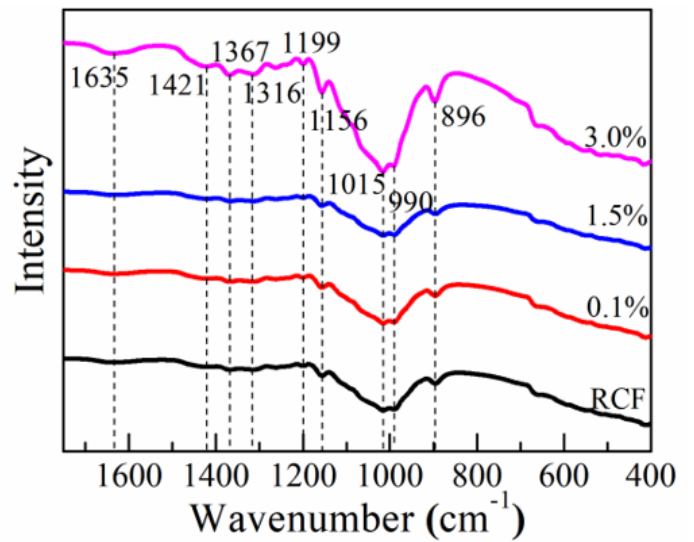
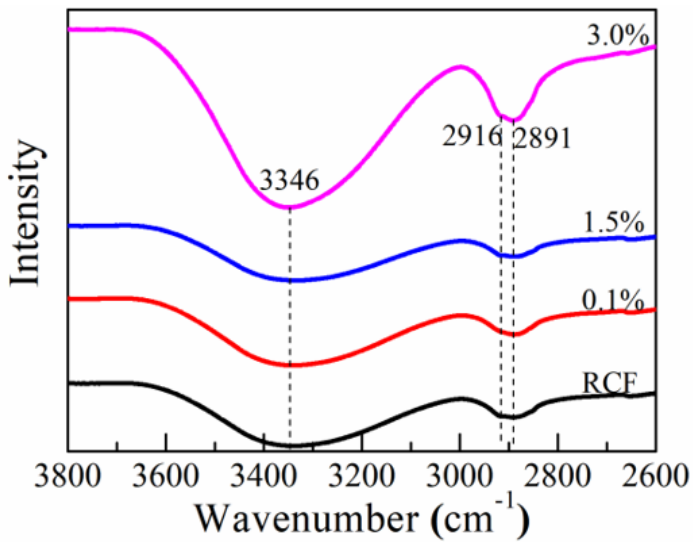


a

b

Figure 4

The FTIR spectrum of ANFs and RCFs which original material came from corn straw and the cellulose were prepared by acid-alkali method a) 3800-2600 cm⁻¹, b) 700-1450 cm⁻¹

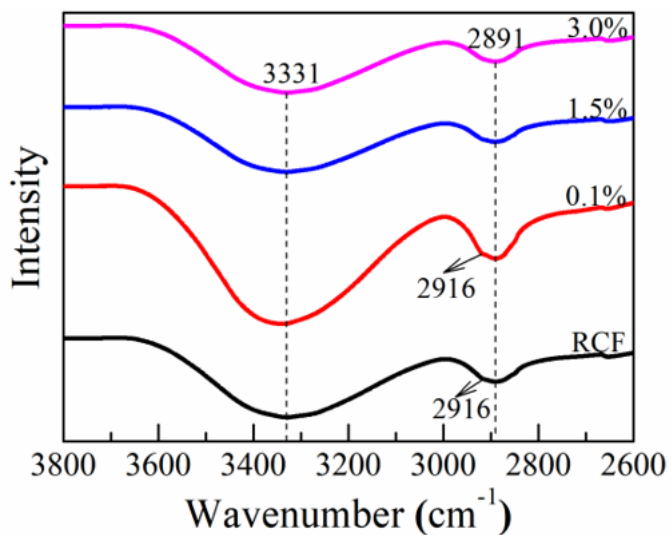


a

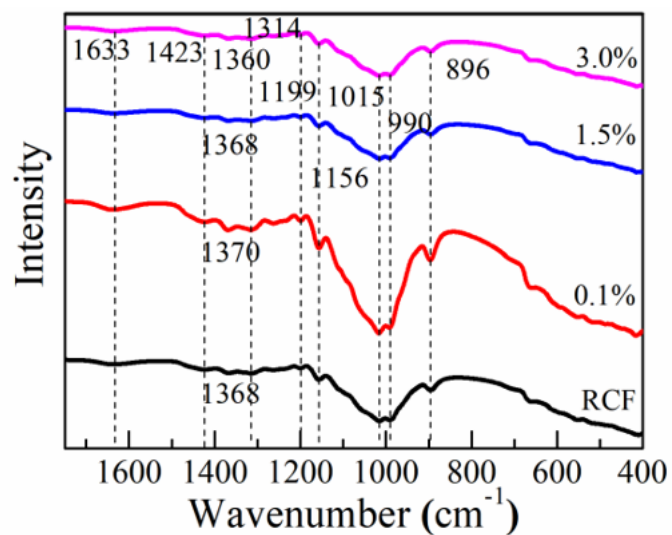
b

Figure 5

The FTIR spectrum of ANFs and RCFs with different concentration nanocellulose and cellulose treated by extracting method from wheat straw a) 3800-2600 cm⁻¹, b) 400-1750 cm⁻¹



a



b

Figure 6

The FTIR spectrum of ANFs and RCFs with different concentration nanocellulose and cellulose treated by acid-alkali method from wheat straw a)3800-2600 cm⁻¹, b)400-1750 cm⁻¹